

On Third Order Resonant Extraction of Protons from a Compact Medical Synchrotron

Steven J. Daley

Submitted to the faculty of University Graduate School

in partial fulfillment of requirements for the

Master of Science Degree

In the Department of Physics

Indiana University

April 2005

Acceptance

Accepted by the Graduate Faculty, Indiana University in partial fulfillment of the requirements for the degree of Master of Philosophy.

Master Committee

A handwritten signature in black ink, appearing to read 'Shyh-Yuan Lee', written over a horizontal line.

Shyh-Yuan Lee, Ph.D.

A handwritten signature in black ink, appearing to read 'Rex Tayloe', written over a horizontal line.

Rex Tayloe, Ph.D.

A handwritten signature in black ink, appearing to read 'Mark Hess', written over a horizontal line.

Mark Hess, Ph.D.

April 2005

Copyright © 2005 by

Steven J. Daley

ALL RIGHTS RESERVED

Acknowledgments

I must thank S. Y. Lee for sharing with me the concepts employed in this accelerator application and I also acknowledge his effort and patience for helping me develop my understanding of this material. A partnership with his knowledge and wisdom enabled me to complete this thesis.

I am grateful for the time and suggestions of the committee members.

I must also acknowledge the support received from the U.S. Particle Accelerator School (USPAS) staff and professors.

I also thank my employer GE Healthcare for their support, enabling me to attend the U.S. Particle Accelerator School classes. I thank Richard Spiering a coworker at GE Healthcare for help with editing.

Abstract

Steven Daley

On 3rd Order

Resonant Extraction

of Protons from a

Compact Medical Synchrotron

The Compact Medical Synchrotron is a source of high-energy protons used for radiation therapy. The CMS extraction systems allow fast or slow extraction for the compact medical synchrotron. Each method of extraction has specific advantages in radiation treatment therapies. The fast-extraction system requires a “kicker,” with fast rise time, and the slow-extraction system uses a third order resonance motion. This thesis examines requirements of efficient extraction systems, delivering dose at controlled exposure rates. Injection, acceleration and extraction requirements are discussed.

Contents

ACCEPTANCE	II
ACKNOWLEDGMENTS	IV
ABSTRACT	V
CONTENTS	6
LIST OF FIGURES	8
LIST OF TABLES	10
1 INTRODUCTION	11
1.1 MOTIVATION.....	11
1.2 ACCELERATOR OVERVIEW	14
1.3 CMS LATTICE.....	17
1.4 EXTRACTION SYSTEM OVERVIEW	19
2 CMS OPERATION	24
2.1 CMS INJECTION.....	24
2.2 CMS ACCELERATION.....	25
2.3 CMS EXTRACTION.....	27
3 MACHINE APERTURES	29
3.1 EMITTANCE OF INJECTED BEAM.....	29
3.2 ADIABATIC DAMPING.....	29
3.3 BEAM WIDTH	30
3.4 APERTURE REQUIREMENTS	32

4	FAST EXTRACTION ELEMENTS	34
4.1	BEAM DYNAMICS.....	34
4.2	CLOSED ORBIT BUMP.....	44
4.3	FAST KICKER.....	49
4.4	VERTICAL LAMBERTSON MAGNETIC SEPTUM.....	52
5	SLOW EXTRACTION ELEMENTS	56
5.1	NON-LINEAR BEAM DYNAMICS.....	57
5.2	RESONANCE DRIVE SEXTUPOLE.....	62
5.3	RF QUADRUPOLE.....	65
5.4	HORIZONTAL ELECTRO-STATIC WIRE SEPTUM.....	70
6	CONCLUSIONS	72
	BIBLIOGRAPHY	74
	CURRICULUM VITAE	76

List of Figures

FIGURE 1 COMPARISON OF PENETRATION RANGE FOR PROTONS AND X-RAYS	12
FIGURE 2 COMPONENT LAYOUT FOR CMS ACCELERATOR	16
FIGURE 3 RATE OF ADIABATIC DAMPING.....	30
FIGURE 4 BEAM SIZE AT INJECTION AND EXTRACTION.....	31
FIGURE 5 INITIAL TRACKING COORDINATES	33
FIGURE 6 CALCULATED BETA FUNCTIONS FOR CMS.....	38
FIGURE 7 OPERATING POINT IN TUNE SPACE.....	40
FIGURE 8 PHASE-SPACE PLOT.....	42
FIGURE 9 SCHEMATIC OF THREE KICK BUMP	45
FIGURE 10 CLOSED ORBIT BUMP	46
FIGURE 11 CLOSED ORBIT BUMP	47
FIGURE 12 CROSS SECTION OF VERTICAL LAMBERTSON MAGNETIC SEPTUM	48
FIGURE 13 FAST EXTRACTION TRAJECTORY.....	50
FIGURE 14 ELEVATION VIEW OF EXTRACTION TRAJECTORY.....	52
FIGURE 17 SLOW EXTRACTION TRAJECTORY.....	56
FIGURE 15 ACTION-ANGLE FORM.....	60
FIGURE 16 SIZE AND ORIENTATION OF SEPARATRIX.....	61
FIGURE 18 RESONANCE DRIVE SEXTUPOLES ACTIVATED.....	64
FIGURE 19 INCREASING QUADRUPOLE STRENGTH.....	66
FIGURE 20 INCREASING SEXTUPOLE STRENGTH	67

FIGURE 21 CHANGING ORBIT RADIUS	67
FIGURE 22 ENLARGING BEAM EMITTANCE.....	68
FIGURE 23 SEXTUPOLE AND RF QUADRUPOLE ACTIVATED	69
FIGURE 24 ELECTRO-STATIC SEPTUM	70

List of Tables

TABLE 1 CMS PHYSICAL PARAMETERS	15
TABLE 2 CMS LATTICE PARAMETERS	17
TABLE 3 SUMMARIES OF APERTURES.....	32
TABLE 4 CLOSED ORBIT BUMP.....	47
TABLE 5 FAST KICKER PARAMETERS	51
TABLE 6 VERTICAL LAMBERTSON MAGNETIC SEPTUM.....	55
TABLE 7 ELECTRO-STATIC SEPTUM PARAMETERS.....	71

1 Introduction

1.1 Motivation

A beam of high-energy protons has many applications in radiation therapy.

Protons have useful properties for treating cancers because the beam deposits its energy mainly at the Bragg peak. Define the Linear Energy Transfer (LET) as

$$LET = dE/dx = \frac{4\pi z^2 e^4 NZ}{mv^2} \left\{ \ln \left[\frac{2mv^2}{I(1-\beta^2)} \right] - \beta^2 \right\} \quad (1.1)$$

where

- e** is the charge of the electron,
- z** is the charge of the projectile ($z=1$ for proton),
- v** is the velocity of the projectile,
- m** is the rest mass of the electron,
- I** is the effective ionization potential of the medium,
- β** is the Lorentz relativistic factor,
- Z** is the atomic number of the absorbing medium,
- N** is the atomic density of the absorbing medium

The average range $\langle R \rangle$ in the absorbing medium is then

$$\langle R \rangle = \int \frac{1}{dE/dx} dE \quad (1.2)$$

Chapter 1 Introduction

Protons deposit almost all their energy in the final 10% of their penetration depth.

This is known as the Bragg peak, as shown in the figure below¹⁸.

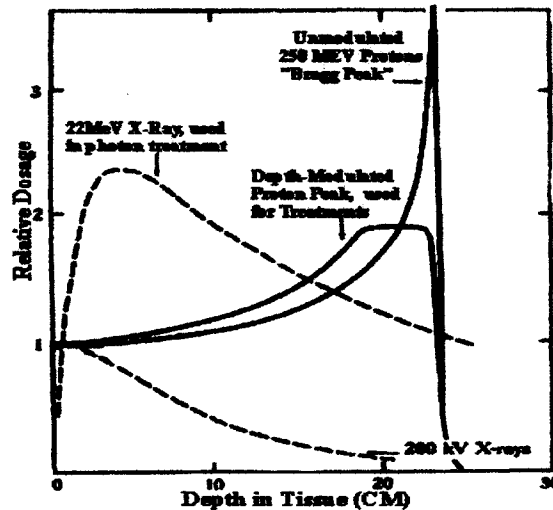


Figure 1 Comparison of penetration range for protons and x-rays

This provides advantage over X or γ -rays by eliminating cancer cells with less harm to healthy cells in its pathway. Indeed, there are many operational proton therapy centers in the world. Some of these centers are Midwest Proton Research Institute (MPRI) at IU, Massachusetts General Hospital in Boston, Loma Linda University Hospital in California, etc.

Protons of 300 MeV attain a penetration depth to 35 cm in a water medium, such as the human body. A typical radiation treatment dose is 3 Gray-liter per minute

$$\frac{3(\text{Gy})(\text{liter})}{(\text{min})} = \frac{3\left(\frac{\text{Joule}}{\text{kg}}\right)(\text{liter})}{(\text{min})} \quad (1.3)$$

Chapter 1 Introduction

We approximate one liter of water is equal to one kilogram,

$$\frac{3(\text{Gy})(\text{liter})}{(\text{min})} = \frac{3(\text{Joule})}{(\text{min})} \quad (1.4)$$

Then the number of 300 MeV particles is

$$Flux_{particles} = \frac{3(\text{Joule})}{(\text{min})} \cdot \frac{1(\text{eV})}{1.602 \times 10^{-19}(\text{Joule})} \cdot \frac{1(\text{particle})}{300(\text{MeV})} = \frac{6.25 \times 10^{10}}{(\text{min})} \quad (1.5)$$

At 300 MeV, this requires 6.25×10^{10} protons delivered to a cancer volume of 1 liter in size per minute. The ramping rate of the CMS can range from 0.5 Hz for slow extraction to 3 Hz for fast extraction. This easily achieves the particle flux requirement for 3 Gray-liters per minute.

Uniformity of the spill is important in delivering a controllable exposure, which can be converted into predictable dose. A technique known as slow resonant extraction is employed to provide a steady stream or “beam” of high-energy protons. The beam is used in a raster-scanning mode with variable energy from pulse to pulse. This thesis studies methods and requirements for efficient extraction of protons from the CMS accelerator.

1.2 Accelerator Overview

The CMS accelerator is a small rectangular synchrotron, incorporating an injection chicane, an RF cavity and two extraction systems into its circumference. We base our design on the successful Cooler Injector Synchrotron (CIS) project at the Indiana University Cyclotron Facility (IUCF).

A pre-accelerated beam of 10 MeV H^- ions is injected into a chicane arrangement of three small dipole magnets. The injected H^- beam merges with the circulating proton beam before passing through a stripper foil where the H^- ions are fully stripped into protons. This phase space painting continues until the desired charge density is reached.

At the maximum field of 1.5 Tesla, dipoles are 3 meters long in order to recirculate a 300 MeV proton into a closed orbit. The single RF cavity provides voltage to accelerate the bunch of protons. The harmonic number is one so RF frequency must match the circulating frequency of the bunch. The proton bunch must fit in one alternation of the RF cycle. Circumference of the CMS ring is 28.5 meters so one RF alternation is about 14.25 meters. The bunch length starts at about 20 meters and the revolution period is about 650 nsec.

Chapter 1 Introduction

Horizontal and vertical betatron tunes determine the operating point. These are determined by the edge angle and bending radius of the dipoles. These tune values can be adjusted with trim quads in order to approach the resonance stopband at the time of beam extraction.

Table 1 lists physical dimensions and beam parameters at injection and extraction energies of the CMS synchrotron.

CMS Physical Parameters		units
Circumference	28.500	m
Machine radius	4.538	m
Dipole length	3.000	m
Dipole rho	1.910	m

Beam Parameters	Injection	Extraction	units
Kinetic Energy	10	300	MeV
momentum	0.137	0.809	GeV/c
velocity	4.37E+07	1.96E+08	m/s
β	0.14479	0.65244	
γ	1.0117	1.32	
$\gamma\beta$	0.1465	0.8614	
Dipole B	0.24	1.41	T
$B\rho$	0.45	2.698	T-m
freq rev	1.28E+06	6.86E+06	Hz
gamma tr	1.393		
$\sigma_x(\text{avg})$	8.9	3.7	mm
$\sigma_y(\text{avg})$	10.9	4.5	mm

Table 1 CMS Physical Parameters

The machine layout is as shown in the figure below.

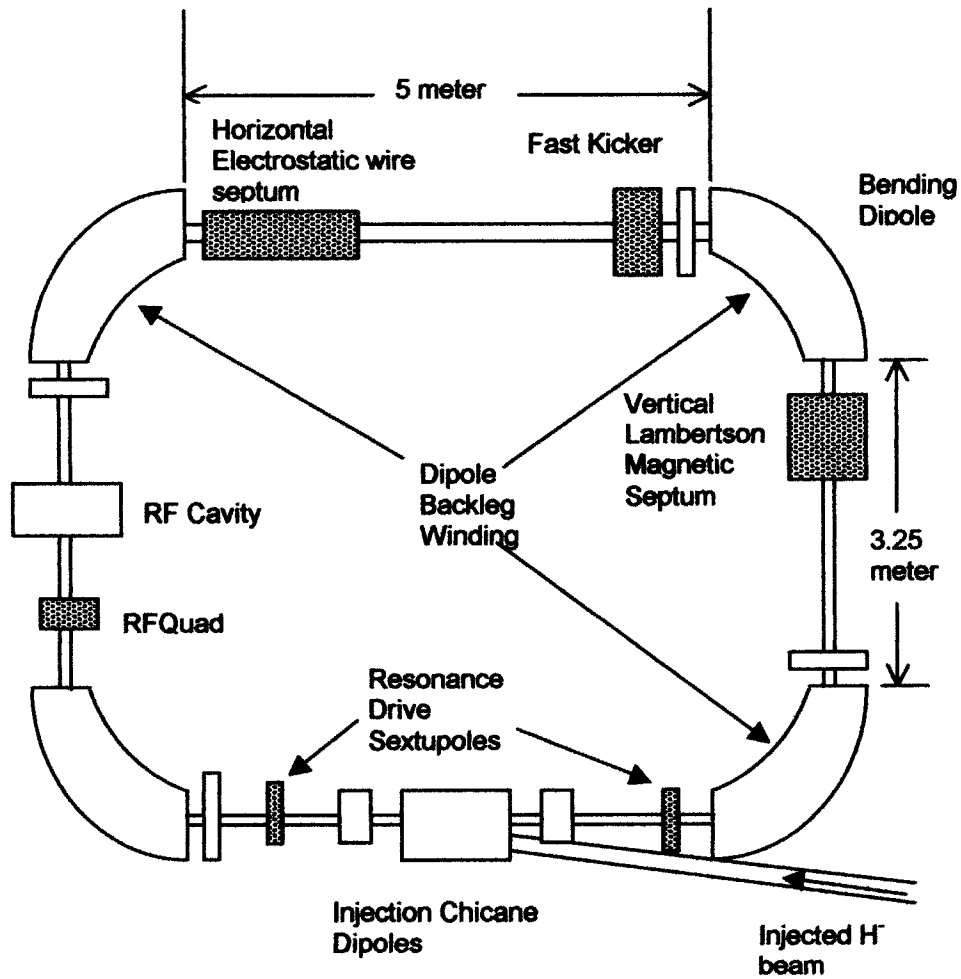


Figure 2 Component layout for CMS accelerator

Shaded elements used for extraction are described in this paper.

1.3 CMS Lattice

The synchrotron lattice design has been optimized by Al Harbi, et al.⁷

Parameter	Symbol	Value	Units
Circumference	C	28.5	Meter
Bend radius	ρ	1.909	Meter
Dipole length	l	3.00	Meter
Dipole Edge Angle	Φ_{edge}	8.5	degree
Injection Energy	E_{inj}	~ 10	MeV
Extraction Energy	E_{max}	~ 300	MeV
Beta functions	β_x	10.4	Meter
	β_y	7.8	Meter
Dispersion	D	2.4	Meter
Tunes	ν_x	1.682	
	ν_z	0.683	
Chromaticities	C_x	-1.14	
	C_z	-0.18	
Transition γ	γ_t	1.393	
p^+ / bunch	N_{bunch}	2×10^{11}	
Admittances	ϵ_x	100	$\pi\text{-}\mu\text{rad}$
	ϵ_z	100	$\pi\text{-}\mu\text{rad}$

Table 2 CMS Lattice parameters

Chapter 1 Introduction

Design of the CMS accelerator has optimized the following parameters:

- Machine circumference of 28.5 meters
- Maximum dipole field of 1.41 T, giving a bend radius $\rho = 1.91$ m.
- Dipole length and edge angles provide focusing to the betatron motion.
- Straight side lengths optimized for maximum energy below transition energy.
- Injection Chicane implemented for multi-turn charge exchange injection.
- Stripper foil used for charge-exchange injection of H^- ions to p^+ .
- RF tuning range equal to circulating frequency, i.e. 1.53 MHz – 6.87 MHz.

1.4 Extraction System Overview

The CMS accelerator employs two methods of beam extraction. The fast extraction system allows efficient tuning of extraction beamline elements, while the slow extraction system allows delivery and control of predictable dose rates. For the extraction process, we implement two different septa for isolating extracted particles from those circulating in the ring. We use a horizontal electrostatic wire septum to deflect selected particles radially outward onto the extraction trajectory where they will encounter the field of the Lambertson magnetic septum. We also use a Vertical Lambertson magnetic septum to deflect particles which are on the extraction trajectory, vertically upward out of the plane of the accelerator.

The fast extraction system extracts the entire bunch in a single revolution. This extraction method would be used for tuning extraction beamline elements and for scanning radiation treatment courses. Since the energy of an extracted synchrotron beam can be changed from pulse to pulse, the scanning radiation has many useful applications. In contrast, the slow extraction system extracts the bunch over many revolutions ($\sim 2 \times 10^7$). This slow spill would allow precise control of radiation therapy doses.

Chapter 1 Introduction

In Chapter 2, we discuss design of the CMS accelerator lattice and its operating cycle. The lattice consists of magnetic elements with constant or linear field gradients, i.e. dipoles and quadrupoles. The dipoles recirculate protons to a fixed closed orbit, while the dipole bending radius and edge-angles provide linear restoring force, needed to confine the beam. Dipole parameters and side lengths determine the horizontal and vertical tunes of betatron motion as well as transition energy of the machine. The Compact Medical Synchrotron (CMS) is designed to accelerate a bunch of protons to 300 MeV or $\gamma = 1.32$. In the CMS, extra effort is placed on designing an optimized extraction system to efficiently deliver a controllable “spill” of protons.

In Chapter 3, we discuss the effect of adiabatic damping on the beam size. During acceleration, the beam experiences a damping force due to the increase in momentum. Apertures of the magnetic septum and the electro-static septum are optimized for the beam size at their locations in the ring.

In Chapter 4, we discuss the design of elements used in the Fast Extraction system. Due to adiabatic damping, we create a closed-orbit bump at the magnetic septum to reduce distance from the beam center to the septum. The dipoles are equipped with extra windings, used to provide a small perturbation to their magnetic fields. These “back-leg” windings create kicks in the orbit with which we use to construct a localized bump in the closed orbit. This “3-kick

Chapter 1 Introduction

bump" is an effective method to move the beam closer to the septum, as beam width shrinks with acceleration.

The magnetic septum has a field free area where the beam can circulate with no effect from the magnetic field. The field free area is separated from the magnetic field area by a thin (1 cm or less) wall, called a septum. In the horizontal field region of the magnetic septum, the extraction trajectory will deflect vertically upward out of the plane of the accelerator.

The circulating beam is deflected onto the extraction trajectory by a fast kicker, which must have a rise time shorter than the gap length of the circulating beam. The extraction trajectory takes the beam into the horizontal field of the magnetic septum, where it is deflected vertically upwards and out of the machine. Possible candidates for the fast kicker are a traveling wave kicker or a fast ferrite kicker.

The fast kicker is uniquely used for the fast extraction process while the electrostatic septum is only used for slow extraction. The magnetic septum and the closed orbit bump are used for both methods of extraction.

In Chapter 5, the method of resonant slow extraction is addressed. Application of resonance drive sextupoles, the RF driven quadrupole and horizontal electro-

Chapter 1 Introduction

static wire septum, are detailed in this section. We introduce Hamiltonian mechanics to facilitate analytical design of the Slow Extraction system.

By using a sextupole to create a nonlinear magnetic field potential, we cause the protons to follow a resonant trajectory. This is seen as a geometric aberration in the phase-space ellipse, distorting the ellipse into a triangle. A separatrix encloses the triangle and defines resonant trajectories between stable and unstable motion.

These resonant trajectories allow gradual displacement of protons to larger radii, where they incrementally step outward across the wires of the electro-static septum. A high-voltage electrode attracts protons radially outward onto the extraction trajectory, leading to the magnetic septum where they are deflected vertically upwards for extraction from the machine.

To achieve a steady output of protons at constant flux, we adjust the sextupole strength such that the stable area is large enough to have no effect on the stored protons. We then use a modulated quadrupole, driven with an RF signal operating at twice the betatron frequency to excite particles onto the separatrix for extraction. The RF quadrupole field creates a chaotic diffusion process for particles near the separatrix. The diffusion process can be controlled by modulation frequency and quadrupole field strength.

Chapter 1 Introduction

We use the computer-tracking program Methodical Accelerator Design⁹ (MAD) to model the CMS accelerator lattice and simulate its performance. The use of MAD allows us to model the beam and accelerator as a dynamic system and explore the non-linear behavior of the beam in the presence of a sextupole and RF quadrupole combination.

In Chapter 6, we summarize our design choices.

2 CMS Operation

2.1 CMS Injection

The operating cycle of the CMS machine starts by setting the dipoles to match the energy of the injected beam. For a well designed and constructed CMS, trim quadrupoles should be set to zero. These trim quadrupoles will be used at extraction for moving the operating point betatron tune near the third order resonance line.

A typical injector consists of an H^- ion source feeding an RFQ followed by a DTL linac to provide a beam of 10 MeV H^- ions. The H^- ion beam is injected into the second magnet of the injection chicane where it merges with the circulating beam of protons, (which were deflected by the first chicane magnet). Upon exiting this second chicane magnet the H^- ion beam encounters a stripping foil, fully stripping the two electrons from the H^- ions leaving protons. The third chicane magnet bends the merged beams back into closed orbit.

This phase space painting continues until sufficient charge accumulates in the ring. For an estimate, with a 2 mA linac source, the number of particles accumulated in 50 turns is approximately 4×10^{11} protons in a bunch. With an injection efficiency of 80%, we should be able to deliver 3×10^{11} particles per

Chapter 2 CMS Operation

pulse. In reality, the space charge effect will dominate injection efficiency. At a space charge tune shift of about 0.25, we expect to be able to accelerate 3×10^{10} particles per pulse.

2.2 CMS Acceleration

In the CMS synchrotron, four dipole magnets recirculate protons through a single RF cavity. The increase in momentum comes from electric fields experienced inside the RF cavity, used to accelerate the bunch of protons. By increasing the magnet strength synchronously with the proton energy, we maintain a constant closed orbit radius while the beam accelerates. The revolution frequency around the ring is

$$f_0 = \frac{\beta c}{C} \quad (2.1)$$

where β is the relativistic Lorentz factor
 c is the speed of light and
 C is the circumference of the ring

From the previous equation, we get 1.58 MHz at injection and 6.87 MHz at extraction. During acceleration the particle kinetic energy varies with time according to⁷

$$E(t) = E_0[\gamma(t) - 1] \quad (2.2)$$

where E_0 is the rest mass for a proton (938 MeV)

Chapter 2 CMS Operation

γ is the relativistic Lorentz factor

From the previous equations, we write the angular frequency as

$$\omega_0 = 2\pi \frac{c}{C} \sqrt{1 - \left(\frac{E_0}{E + E_0}\right)^2} \quad (2.3)$$

The RF frequency is synchronized with the angular frequency and we have

$$\omega_{RF} = h\omega_0 \quad (2.4)$$

The magnetic field is inserted to give⁷

$$\omega_f = 2\pi \frac{hc}{C} \sqrt{\frac{B^2}{B^2 + \left(\frac{mc^2}{ec\rho}\right)^2}} \quad (2.5)$$

where B is the magnetic field strength

c is the speed of light

h is the harmonic number

C is the circumference of the ring

m is the mass of the proton

e is the charge on the proton and

ρ is the dipole bending radius

The dipole strength is related to the particle energy by

$$B(E) = \frac{2\pi}{ecC} \sqrt{(E + E_0)^2 - E_0^2} \quad (2.6)$$

Chapter 2 CMS Operation

For an average of 0.5 μ seconds/revolution, achieving a ramp time of 0.5 seconds will require at least 300 V from the RF system. If the RF cavity provides 500 V, the ramp time can be reduced to 0.3 seconds. These requirements can be met with a triode or tetrode amplifier.

2.3 CMS Extraction

The magnetic septum is preset for proper deflection of a beam with the desired extraction energy. The bunch accelerates to extraction energy by ramping the dipoles and increasing the RF frequency. When the desired energy is reached, the extraction process begins.

The dipoles are equipped with extra "Back-Leg Windings." The back-leg windings of the dipoles are used to create a closed orbit bump at the magnetic septum location. Displacement of this bump is excited only during the time of extraction. Fast extraction uses a fast-rising magnetic kicker to deflect the entire bunch in a single revolution. The rise time must be less than the circulating period at maximum energy, or 145 nsec. The bunch is kicked into the field of the magnetic septum, where it is then deflected vertically upward into the extraction beamline.

Slow extraction relies on a sextupole field to create a non-linear resonance in the beam motion. The sextupole strength is set so the stable area is greater than the emittance of the circulating beam. The RFQ is then driven to enlarge the beam's

Chapter 2 CMS Operation

emittance, pushing particles into the sextupole field where they exhibit resonant motion. This motion causes some particles to cross into the electric field of the electro-static septum. The electro-static field deflects particles onto a trajectory leading into the magnetic field of the septum, where they exit vertically. This “RF knock out” gives precise control of the beam “spill”.

3 Machine Apertures

3.1 Emittance of Injected Beam

Emittance of the beam is defined as the beam width times its angular divergence. The emittance is a constant of the system i.e. it remains unchanged around the ring. Emittance of the injected beam after exiting the stripping foil is conservatively estimated to occupy a phase-space that will be no more than $100 \pi \mu$ meter radians in both transverse dimensions. Using a Gaussian beam approximation for 95 % of the particles, rms emittance of the beam is about $100/6=17 \pi \mu$ meter radians.

3.2 Adiabatic Damping

As the proton bunch accelerates and ramps up its energy, its size decreases due to the changing ratio of transverse to longitudinal vectors. This is seen as the ratio of high-energy to low-energy relativistic factors¹

$$\mathcal{E}_{highenergy} = \sqrt{\frac{\gamma\beta_{highenergy}}{\gamma\beta_{lowenergy}}} \mathcal{E}_{lowenergy} \quad (3.1)$$

where $\gamma = \frac{1}{\sqrt{1-\beta^2}}$ is the Lorentz relativistic velocity factor

$\beta = \frac{v}{c}$ is the Lorentz relativistic velocity factor

Chapter 3 Machine Apertures

As the beam bunch accelerates, it shrinks in size due to adiabatic damping effect.

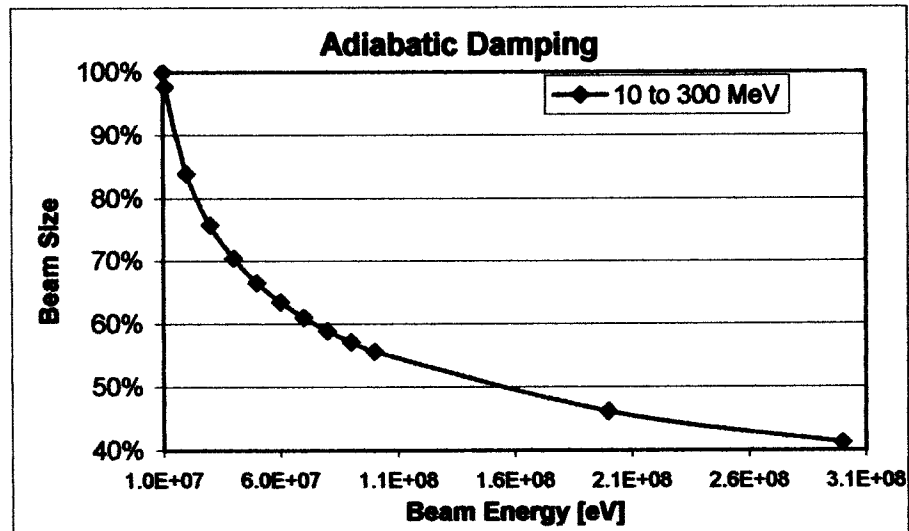


Figure 3 Rate of Adiabatic Damping

This graph shows how the beam shrinks to less than 50% of its initial injection emittance as it accelerates from 10MeV to 300 MeV.

3.3 Beam Width

The transverse size of the beam at any position in the ring depends on the initial beam emittance and the value of the beta function at that position in the ring. The beam half-width (or radius) is given by σ^{11}

$$\sigma = \sqrt{\beta(s)\epsilon} \quad (3.2)$$

where σ rms width of the beam in meters,
 β local beta function in meters and
 ϵ rms emittance in meter radians

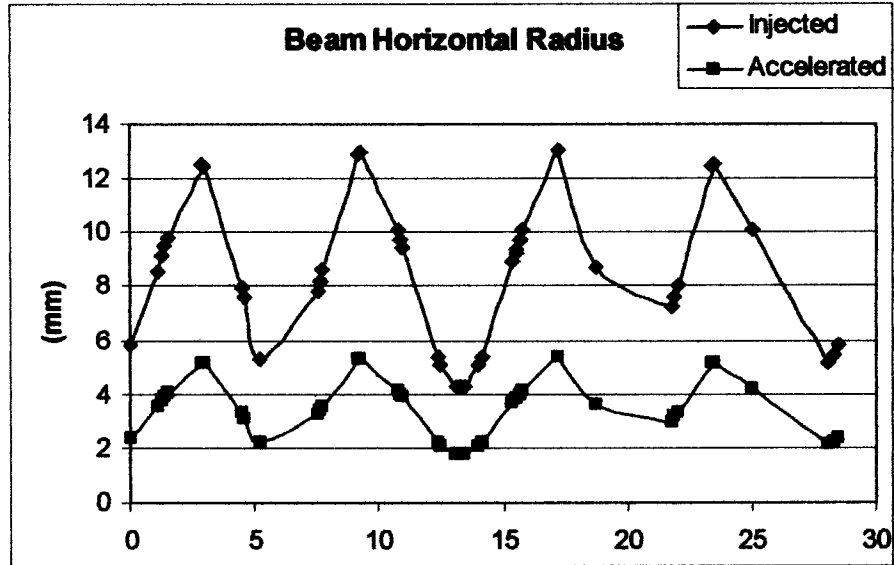


Figure 4 Beam size at injection and extraction

Plot of beam size around the ring from MAD data, abscissa starts at electro-static septum. The effect of the beta function on the beam envelope is revealed, the maximum beam radius is about 13 mm at injection energy.

Chapter 3 Machine Apertures

Aperture Requirements

As a rule, proton accelerators need their full aperture at injection and it is then that their design is most critical. The dipole apertures are 6 cm tall while multipole magnets such as; trim quads, resonance drive sextupoles and RFQ apertures will be 80 mm.

The following table lists beam diameter at critical locations in the ring.

Emittance= 17π mm mrad

Location	Beta _x (m)	E _{beta}	Diameter (mm)	Damping 42%
Injection CB3	1.1	18.32	8.56	3.59
ES Septum	2	33.32	11.54	4.84
Fast Kicker	1.6	26.65	10.32	4.33
Lambertson	3.4	56.64	15.05	6.3

Location	Beta _y (m)	E _{beta}	Diameter (mm)	Damping 42%
Injection CB3	6.3	104.96	20.48	8.60
ES Septum	4	66.64	16.32	6.85
Fast Kicker	3.8	63.30	15.91	6.68
Lambertson	7.9	131.61	22.94	9.63

Table 3 Summaries of Apertures

Chapter 3 Machine Apertures

For tracking simulations in MAD we used a horizontal distribution of ± 30 mm, this is the limiting aperture dimension in the ring.

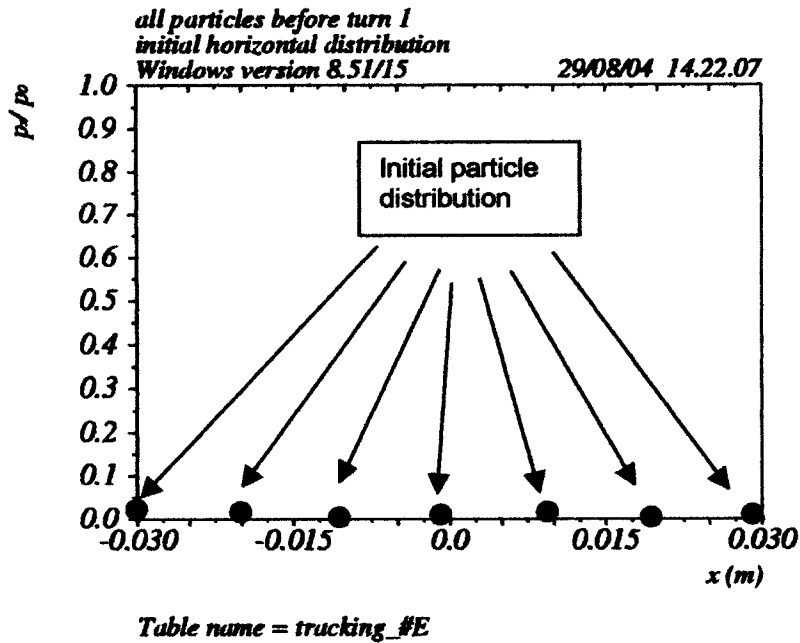


Figure 5 Initial tracking coordinates

Tracking simulation in MAD for initial particle coordinates before tracking. We track these particles around the ring for 100 orbits to simulate the dynamics of extraction.

4 Fast Extraction Method

4.1 Beam Dynamics

The CMS accelerator can increase a protons' kinetic energy to 300 MeV. At extraction, the relativistic momentum increases as the gamma function. In CMS we have

$$\vec{v} = 1.95 \times 10^8 \text{ meters/sec} \quad (4.1)$$

and

$$\vec{p} = m\vec{v}\gamma = 808 \text{ MeV}/c \quad (4.2)$$

where

$$\gamma = \frac{1}{\sqrt{1-\beta^2}} = 1.32 \quad \text{and} \quad (4.3)$$

$$\beta = \frac{v}{c} = 0.652 \quad (4.4)$$

Inside the accelerator the Lorentz force is the only force acting on the proton and is given by the equation

$$\vec{F}_{LORENTZ} = \frac{\Delta\vec{p}}{\Delta t} = q(\vec{E} + \vec{v} \times \vec{B}) \quad (4.5)$$

where

- q is the proton charge,
- E is the electric field
- V is the velocity
- B is the magnetic field

Chapter 4 Fast Extraction Method

Magnetic multipoles of the lattice create potential fields for the particles to traverse. Linear motion of the particle is determined by magnetic fields that are constant or vary linearly with displacement, these are the dipoles and quadrupoles. The linear transverse motion of an ideal particle can be separated into several distinct effects. We identify the closed orbit motion, betatron oscillation and dispersive motion, as shown in the equation below.

$$y(s) = y_{c.o.}(s) + y_{\beta}(s) + D(s)\delta \quad (4.6)$$

where $y(s)$ is the x or z position at location (s)

$y_{c.o.}(s)$ is closed orbit motion

$y_{\beta}(s)$ is the betatron oscillation motion

$D(s)$ is the dispersion function

$$\delta = \left(\frac{p - p_0}{p_0} \right) = \frac{\Delta p}{p_0} \quad (4.7)$$

is the deviation from the design momentum

where p is the momentum of any particle and

p_0 is the momentum of the reference particle

Chapter 4 Fast Extraction Method

Stable motion in a cyclic accelerator must be a closed orbit around the ring.

Dipoles are used to recirculate the beam into the closed orbit. The first term of Equation (4.6) represents motion on the reference orbit. To examine the motion from the reference orbit, it is useful to use distance s along the trajectory as the independent variable instead of time.

$$\frac{d}{dt} = \frac{d}{ds} \frac{ds}{dt} = v \frac{d}{ds} \quad (4.8)$$

This transformation moves our reference frame to that of the ideal particle, where all motion is viewed as small perturbations to the reference orbit. In a bunch of protons there can only be one ideal particle on the reference orbit. Other mono-energetic particles perform small amplitude oscillations around the reference orbit.

The equation of motion is a second order homogeneous differential equation known as Hill's equation. When $K > \text{zero}$, Hill's equation is that of a harmonic oscillator. Particle trajectories are then solutions of Hill's equation. This oscillating betatron motion is described by the equation

$$x''(s) + K(s)x(s) = 0 \quad (4.9)$$

where x represents transverse coordinate

$$K(s) = \left(\frac{1}{\rho^2}(s) - \frac{B_1}{B\rho} \right) \text{ is quadrupole strength,}$$

Chapter 4 Fast Extraction Method

$B_1 = \frac{\partial B}{\partial x}$ is the quadrupole gradient,

$B\rho = \frac{p}{e}$ is the magnetic rigidity of the particle,

p is the particle momentum

e is the proton charge

Quadrupole fields provide the linear restoring force needed to guide particles along the reference orbit. The magnetic field in the current-free region of a quadrupole magnet can be derived from the multipole expansion equation¹

$$B_z + jB_x = B_0 \left(\sum (b_n + ja_n)(x + jz)^n \right) \quad (4.10)$$

where $n = 0$ for dipole, $n = 1$ for quadrupole, $n = 2$ for sextupole, etc.

Concentration of magnetic field lines in a quadrupole increases linearly from the center of the aperture bore. For the quadrupole gradient we have¹

$$B_z = B_0 b_1 x = \left(\frac{\partial B_z}{\partial x} \right)_{x_0} x = B_1 x \quad (4.11)$$

$$B_x = B_0 b_1 z = \left(\frac{\partial B_x}{\partial z} \right)_{z_0} z = B_1 z \quad (4.12)$$

The phase advance ψ relates the period of the betatron oscillation to distance the particle advances, in meters.¹

Chapter 4 Fast Extraction Method

$$\psi = \int \frac{ds}{\beta} \cong \frac{L}{\langle \beta \rangle} \quad (4.13)$$

where ds is the distance change in meters

β is the beta function in meters

The betatron wavelength is given as¹

$$\lambda_\beta = 2\pi \langle \beta \rangle \quad (4.14)$$

Tracking simulation in MAD.

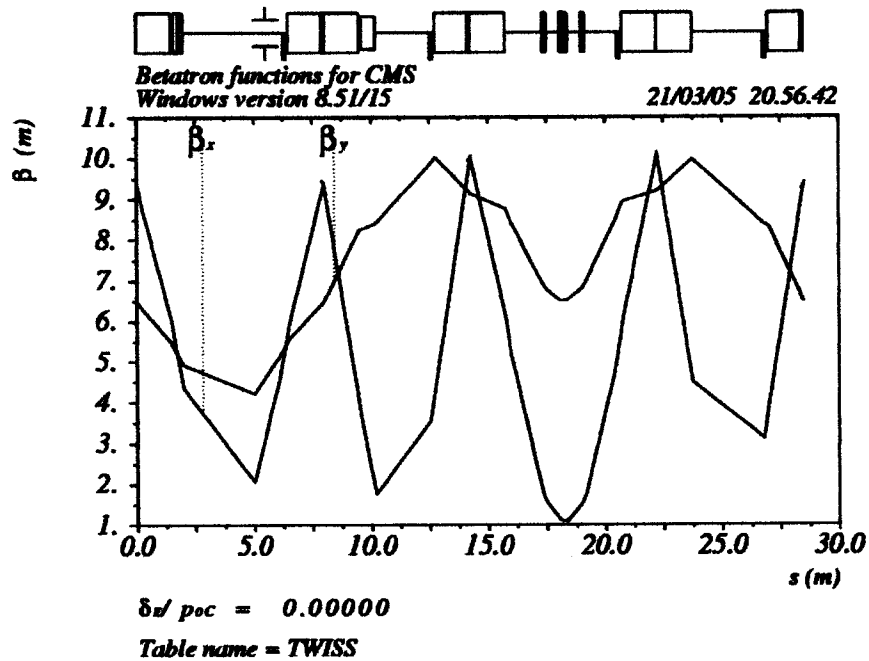


Figure 6 Calculated beta functions for CMS.

Chapter 4 Fast Extraction Method

The quadrupole field gradient creates focusing forces in the ring. The stronger the quadrupole focusing, the greater the betatron phase advances. Number of oscillations per orbit is known as the tune of the betatron motion. The tune is calculated as¹

$$Q_y = \nu_y = \frac{\psi}{2\pi} = \frac{1}{2\pi} \int_s^{s+C} \frac{ds}{\beta_y(s)} \quad (4.15)$$

where β_y is the betatron amplitude function

ψ_y is the betatron phase

Chapter 4 Fast Extraction Method

Horizontal and vertical tunes can be plotted together to represent the Operating point in tune space

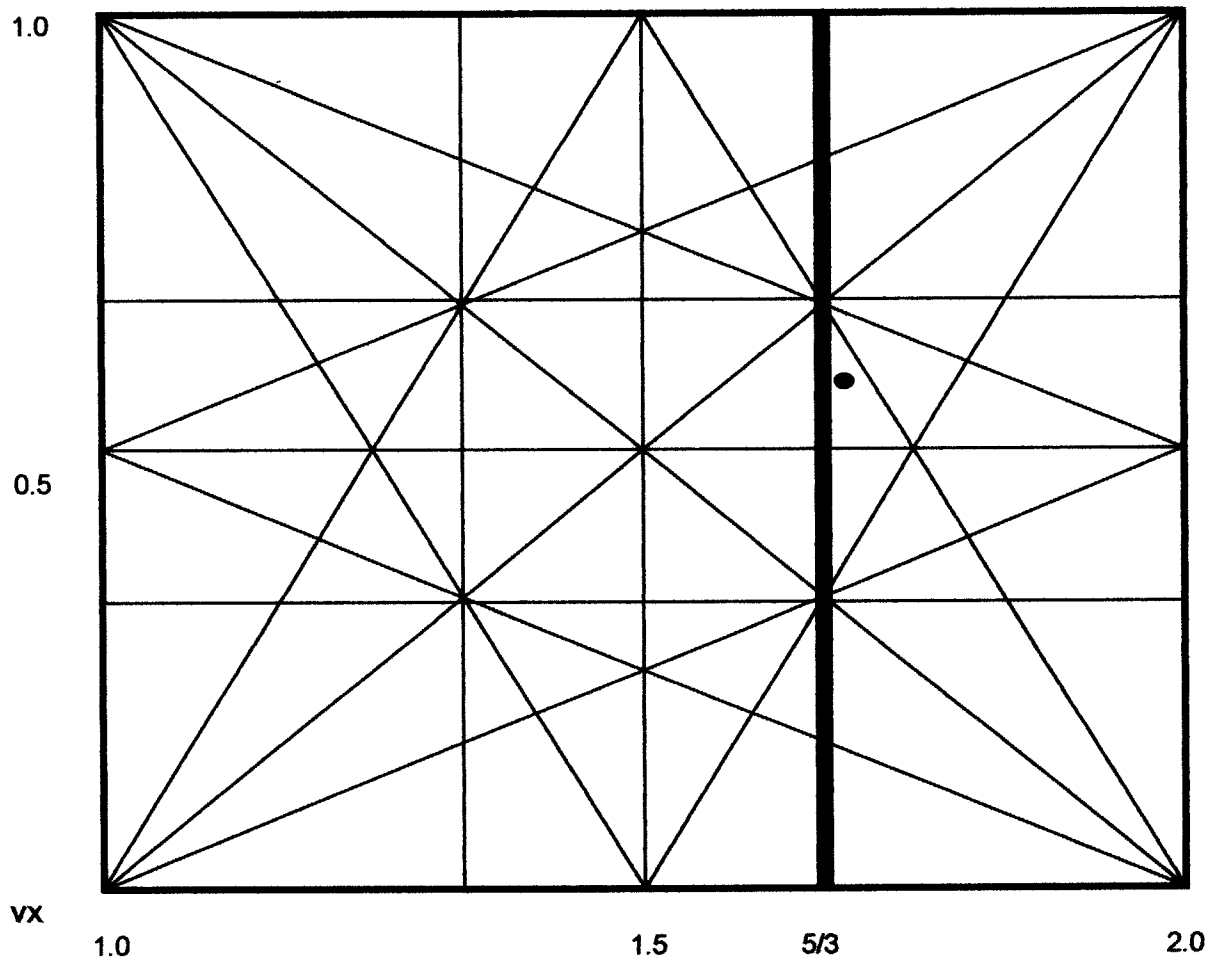


Figure 7 Operating point in tune space

Operating point in tune space, near the horizontal $5/3$ line, used for the slow extraction process. Changing the trim quad strength is a method used to change the betatron tunes of the beam, referred to as the operating point in tune space.

Chapter 4 Fast Extraction Method

When oscillating betatron motion is characterized in phase space, there are two related derivatives of the beta function given below¹⁰

$$\alpha(s) = -\frac{1}{2}\beta'(s) \quad (4.16)$$

$$\gamma(s) = \frac{1 + \alpha^2(s)}{\beta(s)} \quad (4.17)$$

Along with the beta function, they form the Courant–Snyder parameters, also known as the Twiss parameters. These Twiss parameters are related by the equation of an ellipse with a modulus of one

$$\beta\gamma - \alpha^2 = 1 \quad (4.18)$$

Elimination of phase advance from the equations of motion yields an invariant of the motion called the Action J . The invariance is a consequence of Liouville's Theorem, which states that emittance of the beam, is constant around the ring

$$2\pi J = p_0 c \cdot \pi \varepsilon = \text{constant} \quad (4.19)$$

Initial beam emittance determines the phase space area, which remains constant.

Chapter 4 Fast Extraction Method

Tracking simulation in MAD showing cyclic motion of initial distribution.

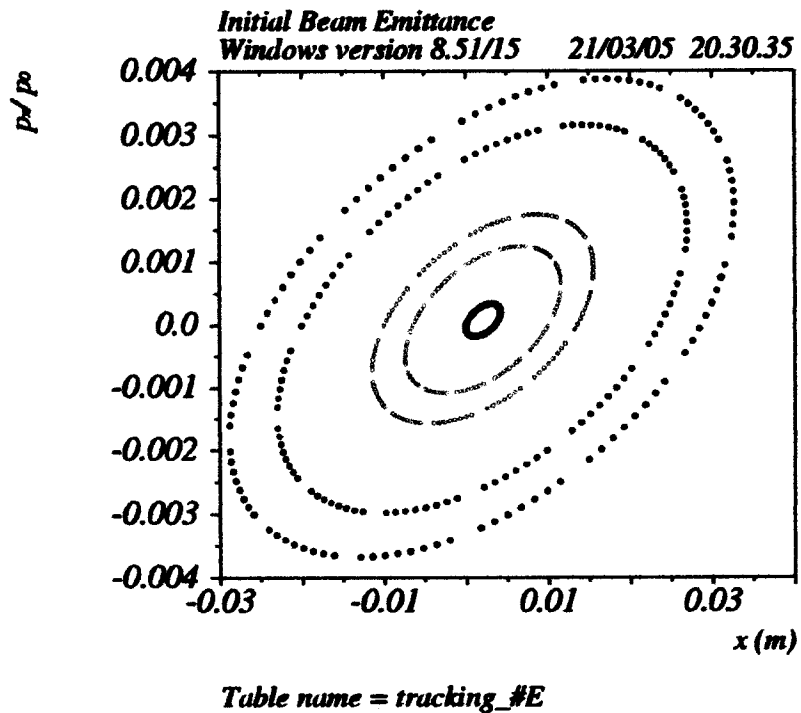


Figure 8 Phase-space plot

Phase-space plot of initial particle distribution for 100 turns.

Many particles in the bunch will have a distribution of momentum around that of the ideal particle. For particles in the bunch that are not at the exact design momentum, there is the effect of Dispersion defined as, “the change in closed orbit as a function of energy.”

Chapter 4 Fast Extraction Method

Dispersion causes "off momentum" particles to have a position distribution perpendicular to the magnetic fields of accelerator elements. This effect is seen as horizontal dispersion in dipoles and as a change in focal length in quadrupoles. The third term in Equation (4.6) represents the off-energy effects.

Chromaticity of the ring is defined as, "the change in tune as a function of energy." This chromatic effect creates a tune spread in the operating point in tune space. Natural chromaticity should be negative to help preserve the waiting beam.

$$C = \frac{dQ}{\delta} \quad (4.20)$$

where $\delta = \frac{\Delta p}{p_0}$ is relative energy error and
Q is the tune

Longitudinal dynamics in the ring are dominated by the electric field produced in the RF cavity. The harmonic number of CMS is one, so the RF frequency must match the particle revolution frequency. Particles in the bunch that are not on the design momentum travel different distances than particles that are on the design momentum. This change in path length with energy is known as momentum compaction. Momentum compaction is defined as the integral of the dispersion¹⁰

$$\alpha_c \equiv \frac{1}{C} \oint \frac{D(s) ds}{\rho} = \frac{\Delta L/L}{\Delta p/p} \quad (4.21)$$

where C is the circumference
 $D(s)$ is the dispersion function
 ρ is the bending radius

Below transition energy, a higher-momentum particle will have a shorter revolution period than the synchronous particle. Above transition energy, a higher momentum particle will have a longer revolution period than the synchronous particle. Transition energy for CMS is¹⁰

$$\gamma_T \equiv \sqrt{1/\alpha_c} = 1.393 \quad (4.22)$$

The CMS accelerator operates below transition energy ($\gamma_{\text{transition}}=1.393$). This avoids the complication of negative mass instability that can cause longitudinal emittance blow up. This simplifies machine operation by increasing the threshold for microwave instability and improving longitudinal stability.

4.2 Closed Orbit Bump

After accelerating to desired energy, the horizontal dimension of the accelerated beam will be reduced by about 50%, due to adiabatic damping. Beam orbit will be manipulated to reduce the strength requirements of the fast kicker.

Chapter 4 Fast Extraction Method

A “three-kick” closed-orbit bump will be used to move beam orbit closer to the Lambertson Magnetic Septum. Back-leg windings in three of the dipoles are used to create this closed-orbit bump, located at the Lambertson Septum.

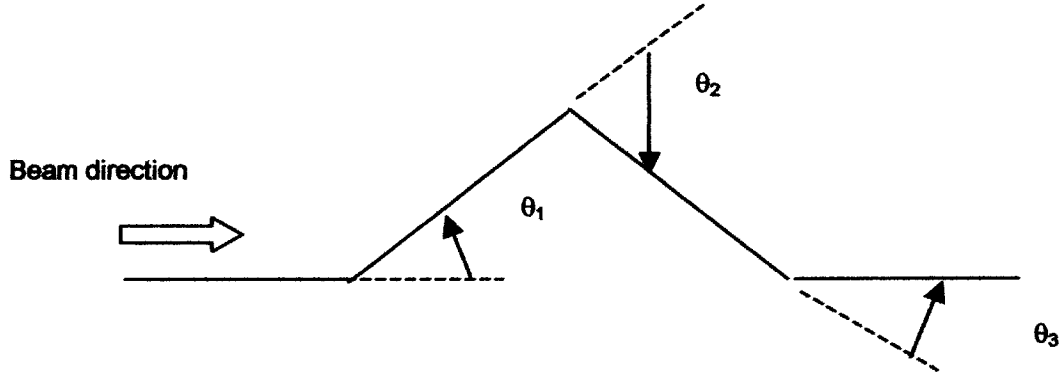


Figure 9 Schematic of three kick bump

Magnitude of the “bump” is determined by the lever arm and the angle θ_1 . The kick angles are related by the formulae¹

$$\theta_2 = -\theta_1 \sqrt{\frac{\beta_1 \sin \psi_{31}}{\beta_2 \sin \psi_{32}}} \quad (4.23)$$

$$\theta_3 = \theta_1 \sqrt{\frac{\beta_1 \sin \psi_{21}}{\beta_3 \sin \psi_{32}}} \quad (4.24)$$

where θ_1 , θ_2 and θ_3 are the kick angles

β_1 , β_2 and β_3 are beta functions at the kickers

ψ_{21} , ψ_{31} and ψ_{32} are phase advance between kickers

Tracking simulation in MAD of the “3-kick” closed-orbit bump created by energizing back leg windings in three of the dipole magnets.

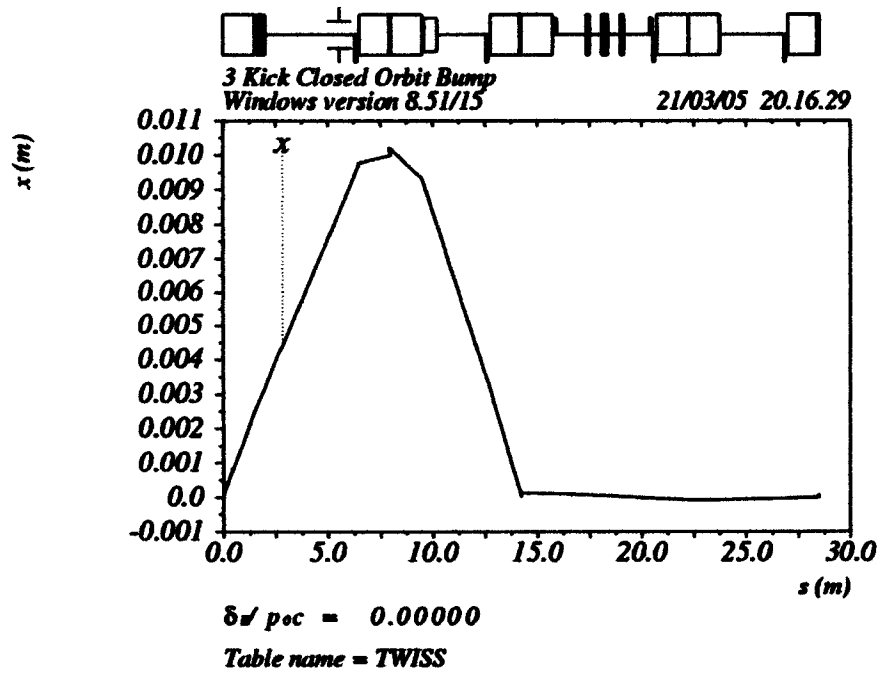


Figure 10 Closed Orbit Bump

We see the orbit has a localized bump but is almost zero elsewhere

Chapter 4 Fast Extraction Method

Kick angle	Excel Calculated	MAD Simulated	units
delta x	11	11	[mm]
theta 1=	1.97	1.8	[mrad]
theta 2=	3.90	3.6	[mrad]
theta 3=	2.49	2.34	[mrad]

Table 4 Closed orbit bump

Calculated angles compare well to simulated angles for the “3-kick” bump. The simulated values were 6% to 9% lower than the calculated values as shown above.

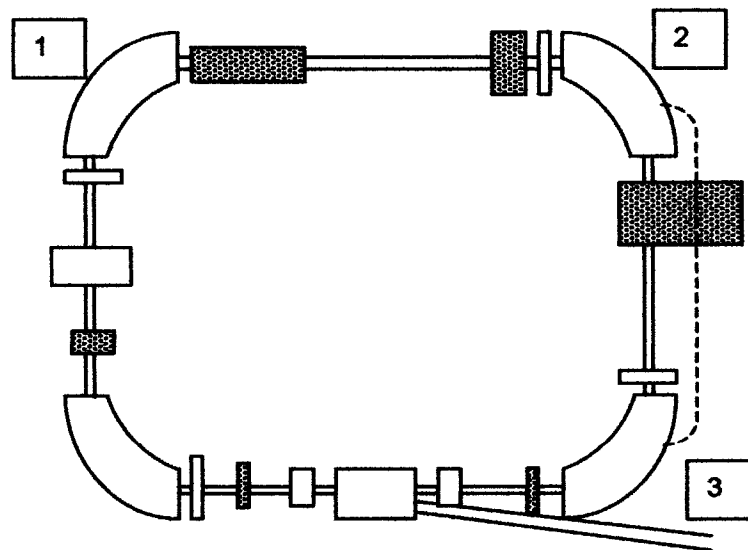


Figure 11 Closed orbit bump

Three dipoles used for closed orbit bump, shown as dotted line.

Chapter 4 Fast Extraction Method

A three-kick closed orbit bump is used to move the circulating beam from position A to position B, as shown in the following cross sectional schematic of the magnetic septum.

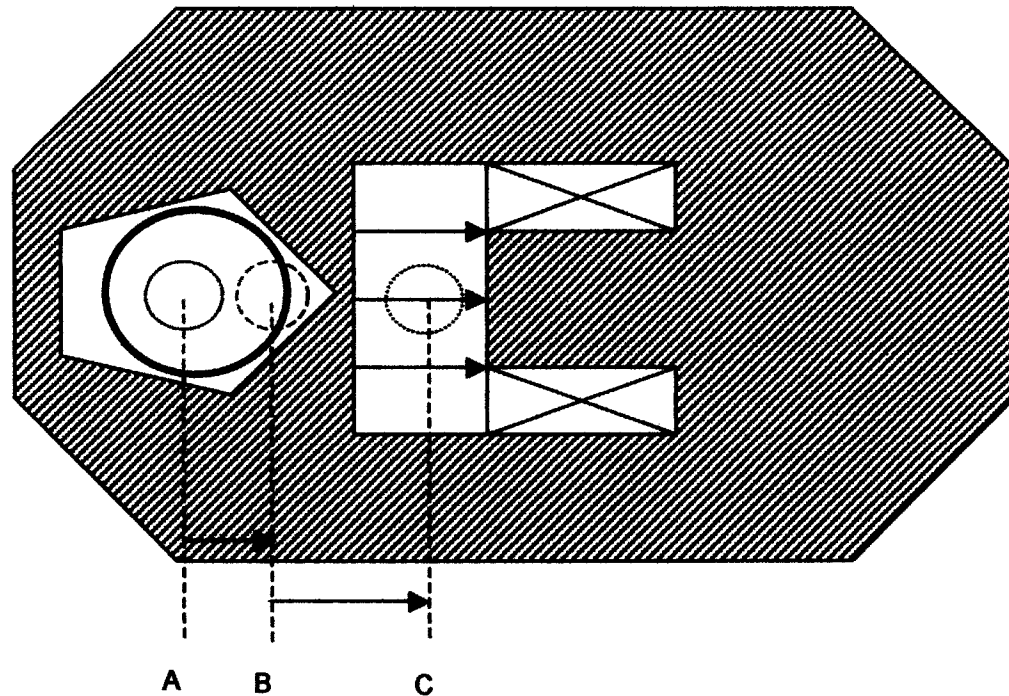


Figure 12 Cross section of vertical Lambertson magnetic septum

Cross sectional diagram of the vertical Lambertson magnetic septum showing beam positions during extraction.

Centerline for the injected beam is at A (large dark ellipse). After accelerating to higher energy, beam dimensions shrink due to adiabatic damping (smaller solid

Chapter 4 Fast Extraction Method

ellipse). The closed orbit bump moves the beam from A to B (smaller dashed ellipse). The fast kicker moves the beam from B to C (smaller dotted ellipse).

From table 2, the field free aperture of the magnetic septum is 15 mm by 23 mm. After acceleration, the bunch is adiabatically damped to about 50%. The local bump must be approximately 11 mm. Extraction efficiency is the fraction of particles that are extracted to the number of particles that are lost by hitting the septum.

4.3 Fast Kicker

The lever arm determines field strength needed to create the deflection angle of the fast kicker. The fast kicker "lever arm" L depends on the beta functions at the kicker and the vertical Lambertson magnetic septum and phase advance between them, this is also true for the horizontal electro-static wire septum. To reduce kicker strength, betatron phase advance between the kicker and magnetic septum should also be close to $\pi/2$, due to $\sin(x)$ dependence. In addition, horizontal betatron amplitude β_x should be maximized at the kicker and septum locations.

We give the stronger lever arm to the electro-static wire septum because its electric field is limited by electrical breakdown in the form of sparking¹.

$$L = \sqrt{\beta_{kicker} \beta_{septum}} \sin \psi_{kicker-septum} \quad (4.25)$$

Chapter 4 Fast Extraction Method

Displacement needed at the magnetic septum is equal to two times the radius of the dampened beam plus the septum width, or about 22 mm.

The kick angle depends on the lever arm and the displacement. The deflection angle is given by¹

$$\theta = \frac{x}{\sqrt{\beta_x(s_k)}\beta(s)\sin\phi_x} = \frac{x}{Lever_Arm} \quad (4.26)$$

The fast kicker sends the entire circulating bunch onto the extraction trajectory and into the field of the magnetic septum as shown below.

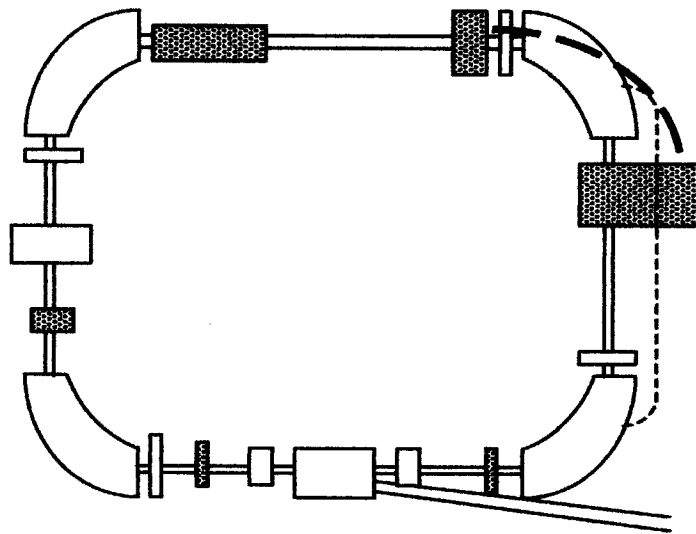


Figure 13 Fast extraction trajectory

Fast extraction trajectory shown as dark dashed line.

Chapter 4 Fast Extraction Method

A summary of parameters fast kicker

Fast Kicker		
length	0.4	[m]
delta x	20.69	[mm]
Phase advance	0.91	[Radian]
Lever Arm	2.081	[m]
theta	9.938	[mrad]
B	0.066	[Tesla]
	668.1	[Gauss}
NI	30958	[AmpTurns]
tums	100	
current	309.58	[Ampere]
t_{rise}	<145	[nsec]

Table 5 Fast Kicker Parameters

4.4 Vertical Lambertson Magnetic Septum

The magnetic septum will be used to deflect all extracted particles up and out of the plane of the circulating beam. After examining the cross section in Figure 12, we examine the transverse motion in figure below.

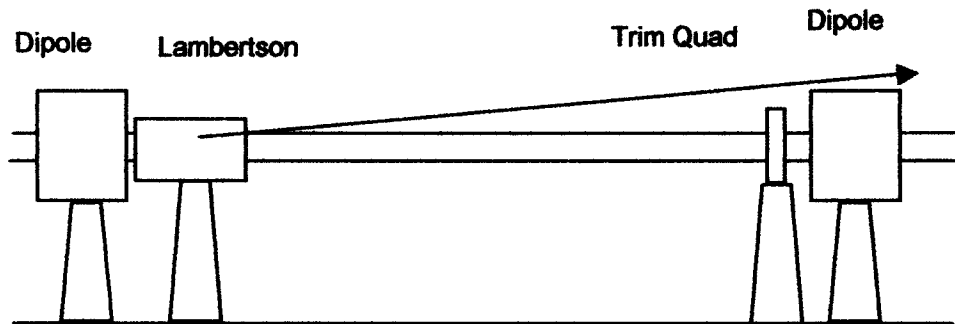


Figure 14 Elevation view of extraction trajectory

View from inside the ring showing magnetic septum and extraction trajectory.

Chapter 4 Fast Extraction Method

The angle of deflection is determined by¹:

$$\theta = \frac{x}{\sqrt{\beta_x(s_k)\beta(s)} \sin \phi_x} = \frac{x}{Lever_Arm} \quad (4.27)$$

where:

- x is displacement needed at the magnetic septum
- $\beta_x(s_k)$ is betatron amplitude at the kicker location
- $\beta_x(s)$ is betatron amplitude at the magnetic septum location
- ϕ_x is betatron phase advance from the kicker location to the magnetic septum location

From Table 4 we determine the displacements needed at the Lambertson septum to be approximately 10 mm. Beta functions are as shown in Figure 6 and phase advance is calculated in MAD. This gives a deflection angle of 244 mrad, we use 250 mrad in our design calculations.

Chapter 4 Fast Extraction Method

The magnetic septum deflects a 300 MeV proton upward by 250 mrad, onto the extraction trajectory. Strength of the magnetic field is determined by magnetic rigidity of the beam, deflection angle and magnet length. The relationship is as follows:

$$\theta = \frac{Bl}{B\rho} \quad (4.28)$$

where θ is deflection angle,
 $B\rho$ is magnetic rigidity,
 B is magnetic field and
 l is magnet length

For a magnet of 0.5 meters length, we need a magnetic field of at least 1.32 Tesla. This field strength can be created by the proper number of turns of wire and necessary current, as shown in the following equation

$$B = \frac{\mu_0 NI}{g} \quad (4.29)$$

where μ_0 is the permeability of free space,
 N is the number of turns,
 I is current and
 g is gap distance

Chapter 4 Fast Extraction Method

The following table lists design parameters for Vertical Lambertson Magnetic septum.

Lambertson Position Data		
distance	3	meters
delta y	0.75	meters
theta	0.245	rad
	14.03	degrees
Lever Arm	3.00	meters
Lambertson Magnet data		
length	0.5	meters
gap	0.03	meters
B	1.317	Tesla
NI	31452	amp-turns
turns	100	
current	314.5	Amperes

Table 6 Vertical Lambertson Magnetic septum

Phase advance is not used for the magnetic septum because extraction trajectory is out of the closed orbit of the ring. The lever arm is then the total length of the drift space from the fast kicker. For an estimated 100 turns and a 30 cm gap we will need 314.5 amps from our power supply.

5 Slow Extraction Method

The technique of slow resonant extraction is used at many pulsed accelerators to increase extracted beam duration. The slow extraction system will extract the single circulating bunch of protons, over many revolutions. A typical extraction spill is on the order of 1-2 seconds, or $\sim 10^7$ revolutions. For a 1-second ramp time, this gives a spill duty cycle of $\sim 60\%$.

The trim quads shift the tune closer to the $5/3$ value. The sextupoles drive the resonance, which distorts the phase-space enclosing the stable ellipse. The rf quadrupole drives the betatron motion onto the separatrix, where particles step to larger amplitude until they cross the wires of the electro-static septum. Slow extraction trajectory is shown as dark dotted line below.

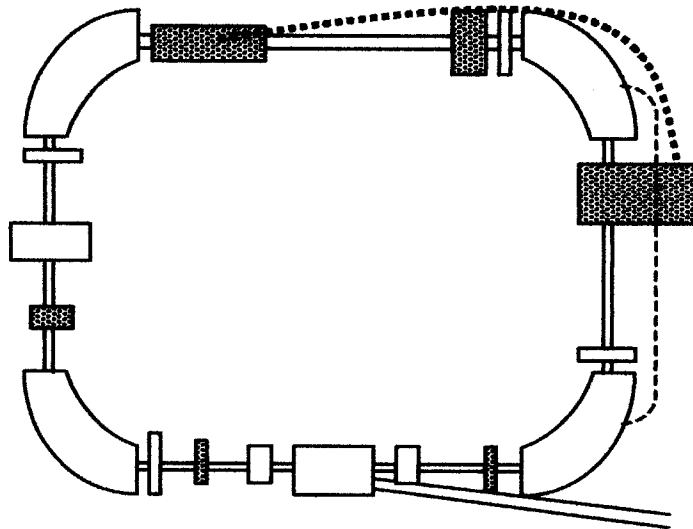


Figure 15 Slow extraction trajectory

5.1 Non-Linear Beam Dynamics

Together the proton and accelerator are viewed as a classical system with constraints, in which dissipative forces can be ignored. With Hamiltonian formalism, we can analytically evaluate the motion of a proton in the accelerator.

The Hamiltonian is equivalent to the total energy of the system; i.e. sum of the kinetic and potential energies.

$$H = T + V \quad (5.1)$$

where T is kinetic energy and
 V is potential energy

Proton momentum provides kinetic energy while magnetic multipoles provide the potential fields of the system. The Hamiltonian describes an evolutionary trajectory in the phase-space of the system. We evaluate the Hamiltonian of transverse motion, working in phase space coordinates and applying canonical transformations to the coordinate system to examine linear and non-linear dynamics of the proton motion.

For particle motion in an accelerator, the Hamiltonian becomes¹

$$H = \frac{y'^2}{2} + \frac{K(s)y^2}{2} \quad (5.2)$$

Chapter 5 Slow Extraction Method

where y and y' are conjugate coordinates ,

$$K(s) = \frac{1}{\rho^2} - \frac{B_1(s)}{B\rho} \quad \text{is the normalized focusing gradient}$$

$$B_1(s) = \frac{\partial B_z}{\partial x} \quad \text{is the quadrupole strength}$$

From this Hamiltonian we can derive the linear equation of motion as an example of a Simple Harmonic Oscillator¹

$$x'' + K(s)x = 0 \quad (5.3)$$

where $K(s) = \frac{1}{\rho^2} - \frac{B_1(s)}{B\rho}$ is the normalized focusing gradient,

$$B_1(s) = \frac{\partial B_z}{\partial x} \quad \text{is the quadrupole strength}$$

x represents horizontal betatron motion and

s represents distance along the orbit

The Vector potential of a sextupole field is given by¹

$$A_x = A_z = 0, \quad A_s = \frac{B_2}{6} (x^3 - 3xz^2) \quad (5.4)$$

where $B_2 = \frac{\partial^2 B_z}{\partial x^2} \Big|_{x=z=0}$

Chapter 5 Slow Extraction Method

The driven non-linear equation of motion in the presence of a sextupole is then¹

$$x'' + K(s)x = -\left[\frac{B''(s)}{2B_0\rho}\right]x^2 \quad (5.5)$$

where, x represents horizontal betatron motion,
 s represents distance measured along the orbit,
 $k(s)$ represents the normalized focusing gradient,
 $\left[\frac{B''(s)}{2B_0\rho}\right]$ represents normalized sextupole strength,
 $B_0\rho$ represents magnetic rigidity of the particles

The sextupole potential field is a periodic function of accelerator circumference, so its effect may be evaluated by the Floquet Analysis.

Floquet transformation converts a linear periodic time varying system into a linear time invariant one. The Floquet transformation maps trajectories of linear unperturbed motion onto a normalized circle so the non-linear motion can be discerned.

Chapter 5 Slow Extraction Method

Pseudo-harmonic betatron motion is normalized to represent simple harmonic motion, by changing the independent variable to the phase advance ψ . This changes the phase space ellipse into a circle in normalized phase space coordinates or Action-angle form. Changing to dimensionless variables we have

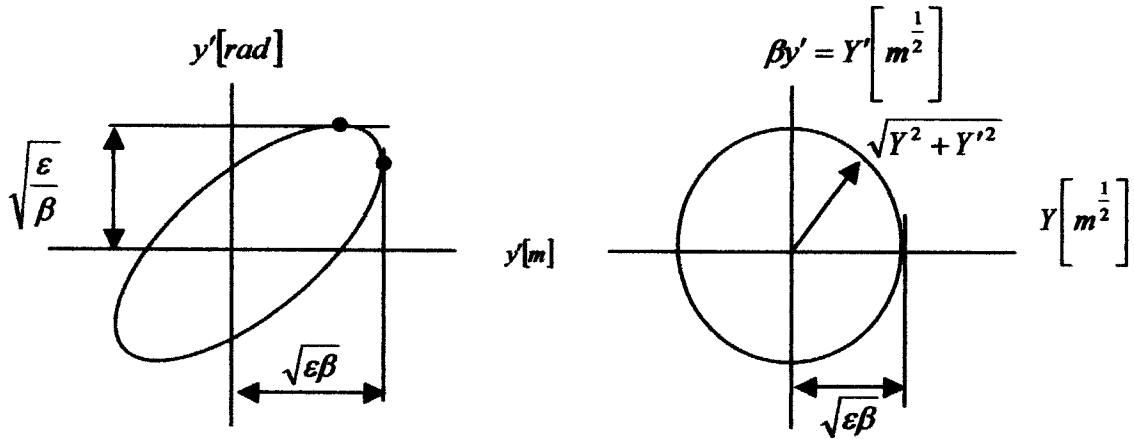


Figure 16 Action-angle form

Phase-Amplitude Form of Solution to Hill's Equation gives the equation of an ellipse in (y, y') phase space.

The complete Hamiltonian including the potential of the sextupole perturbation is¹

$$H = \frac{1}{2} [x'^2 + K_x(s)x^2 + z'^2 + K_z(s)z^2] + \frac{S(s)}{6} [x^3 - 3xz^2] \quad (5.6)$$

where $S(s) = -\frac{B_z}{B\rho}$ is the normalized sextupole strength

Chapter 5 Slow Extraction Method

The first term of the new Hamiltonian describes linear motion as the equation of a circle. The second term is the perturbed motion, created by the resonance sextupole in the horizontal plane of extraction. This new Hamiltonian is used to evaluate stable points, given by zero flow in phase space.

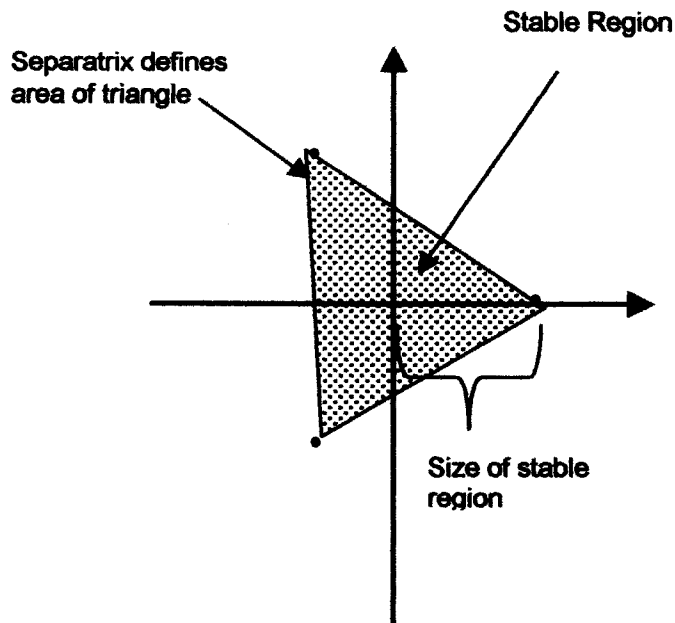


Figure 17 Size and Orientation of separatrix

Corners of the triangle are stable points, which define the orientation of the separatrix. Size of the stable triangle is determined by sextupole strength and the difference between the tune of the particle and the resonance. Liouville's theorem says the size of the stable triangle remains the same in normalized phase space at all locations around the ring. The whole phase-space diagram rotates as the beam moves downstream.

5.2 Resonance Drive Sextupole

The circulating beam is brought into resonant motion, when tune values satisfy¹⁶

$$l\nu_x + m\nu_y = n \quad (5.7)$$

where l, m, n are integers and $n > 0$

If l & m are both non-zero, there is coupled motion in the transverse plane. By setting m equal to zero, vertical motion is unaffected and horizontal motion can be unbound. When a particle exactly repeats its motion every 3 turns, it is called a third order resonance. In a third-order resonance, motion gets unstable when the tune approaches a multiple of one-third.

$$3\nu_x = n \quad (5.8)$$

where ν_x is the fractional part of the betatron tune and n is an integer, 5 for the CMS.

During injection and acceleration, we have taken special efforts to keep tune values of the betatron motion away from the destructive 1st and 2nd order resonances created by the linear potentials. In order to facilitate the slow extraction process, we will be operating with tune values very close to the non-linear resonance created by the sextupole potential. Protons can exhibit resonant motion if their trajectories are exposed to non-linear magnetic fields, such as those created by sextupoles and the tune is near the third integer.

Chapter 5 Slow Extraction Method

Sextupoles create a non-linear geometric aberration to the betatron motion. The phase-space ellipse becomes distorted into a triangle defined by a separatrix. Protons on the separatrix are able to move to larger betatron amplitudes. This non-linear motion is used to deflect particles into the field of the electro-static septum, to be extracted from the closed orbit.

For CMS extraction we consider only the resonance condition when $3\nu_x = 5$. With the Fourier transformation of our Hamiltonian, we extract the 5/3-resonance amplitude $G_{3,0,5}$ given as¹

$$G_{3,0,5}e^{i\psi} = \frac{\sqrt{2}}{24\pi} \oint \beta_x^{3/2} S(s) e^{i[3\chi_x(s) - (3\nu_x - 1)\theta]} ds \quad (5.9)$$

where β_x is the local betatron amplitude function

$S(s)$ is the normalized sextupole strength

$$\chi(s) = \int_0^s \frac{ds}{\beta} \quad \text{is phase advance of the triangle}$$

ν_x is the horizontal tune and

θ is the orbiting angle

The separatrix is maintained, slightly larger than the emittance ellipse of the stable beam. Sextupole drive strength depends on tune difference, beam emittance and the distance from the beam centerline to the electro-static septum

Chapter 5 Slow Extraction Method

wires. We set sextupole strength $S(s)$ based on the equation for the "radius" of the triangle¹

$$J_x = \left(\frac{2\delta}{3G_{3,0,5}} \right) \quad (5.10)$$

Non-linear aberration of phase-space ellipse.

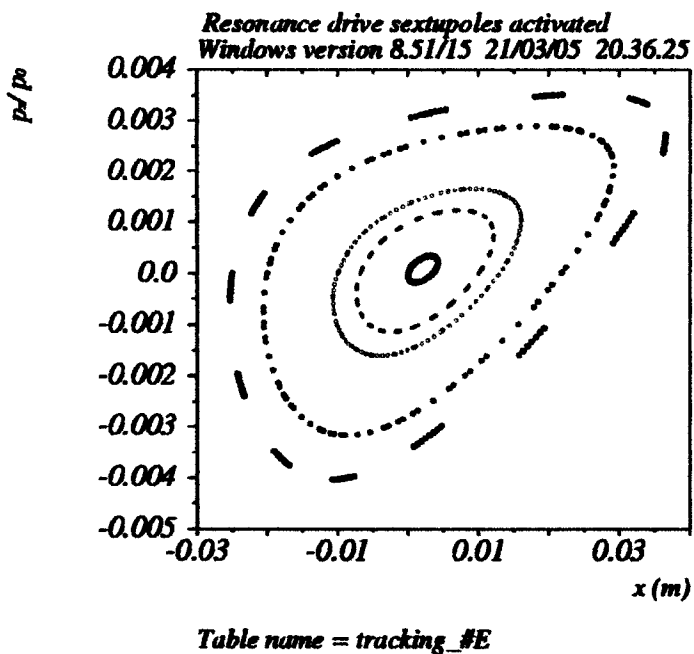


Figure 18 Resonance drive sextupoles activated

Figure shows the phase-space ellipse distorted by application of the sextupole field. All particles are stable at this drive level.

Chapter 5 Slow Extraction Method

Resonance drive Sextupoles are placed in low-dispersion locations so they don't change the chromaticity during the extraction cycle. Multiple-drive sextupoles are spaced $\frac{2\pi}{3}$ apart in betatron phase advance to aid each other.

5.3 RF Quadrupole

For slow extraction from the synchrotron, some of the protons in the bunch must be selected. We examine several physical methods for ion selection, each with different characteristics.

The circulating beam must be made to encounter the stopband of the third-integer resonance in a controlled manner. The tune can be changed with quadrupoles or the beam can be moved radially with RF or dipoles. Stopband width of the resonance can be increased with a sextupole or emittance of the beam can be increased stochastically.

The Steinbach diagram plots circulating beam and resonance together, in amplitude-momentum space. The x-axis is the momentum deviation with respect to the central orbit, which can also be the x-position in dispersive regions or horizontal tune. The y-axis is the normalized amplitude of the particle emittance. With this diagram we compare the ion selection methods described.

Chapter 5 Slow Extraction Method

The following three diagrams are included to illustrate alternate methods which have been employed in previous resonant extraction systems. These methods have the disadvantage that they vary one or more of the lattice elements during the extraction process.

Varying the trim quadrupoles moves the tune of the beam into the resonance.

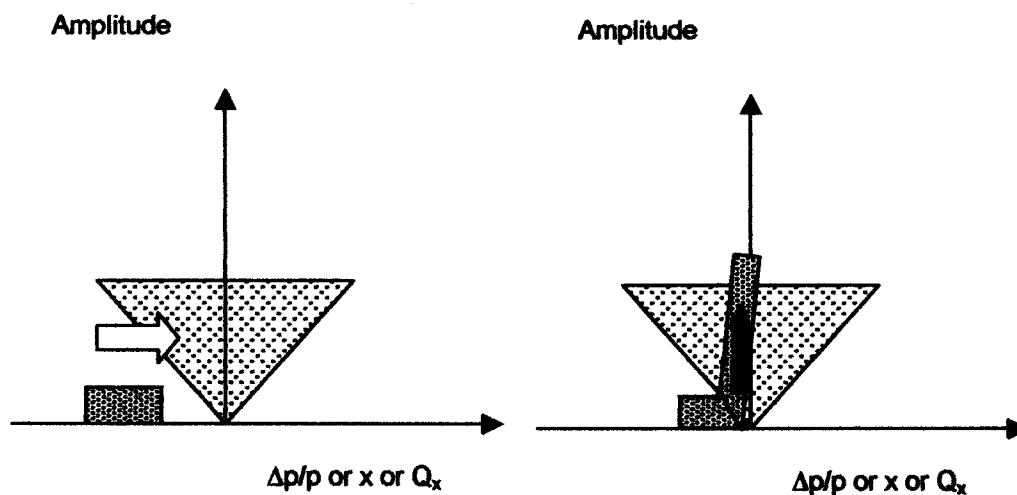


Figure 19 Increasing quadrupole strength

The quadrupoles can be varied to move the tune of the beam into the resonance. The beam is shown as having a large momentum spread and reduced betatron amplitude.

Chapter 5 Slow Extraction Method

Increasing sextupoles increases the stopband width of the resonance.

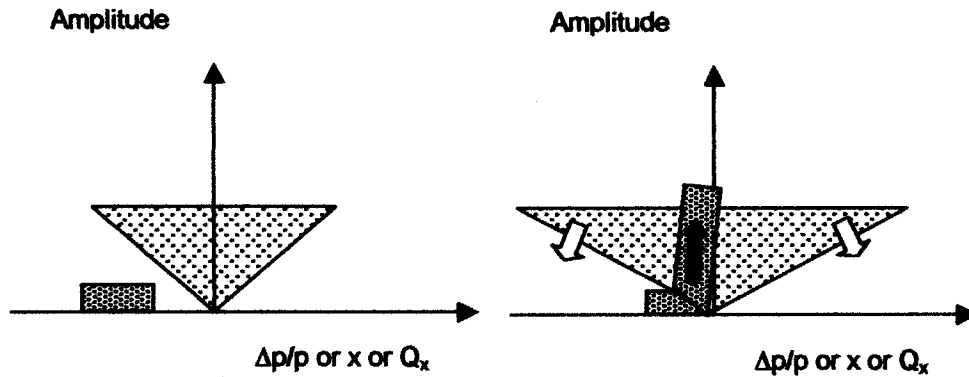


Figure 20 Increasing sextupole strength

The beam is shown as having a large momentum spread and reduced amplitude.

The closed orbit can be shifted radially with dipoles or RF gymnastics to cause the beam to encounter the resonance at a different radius.

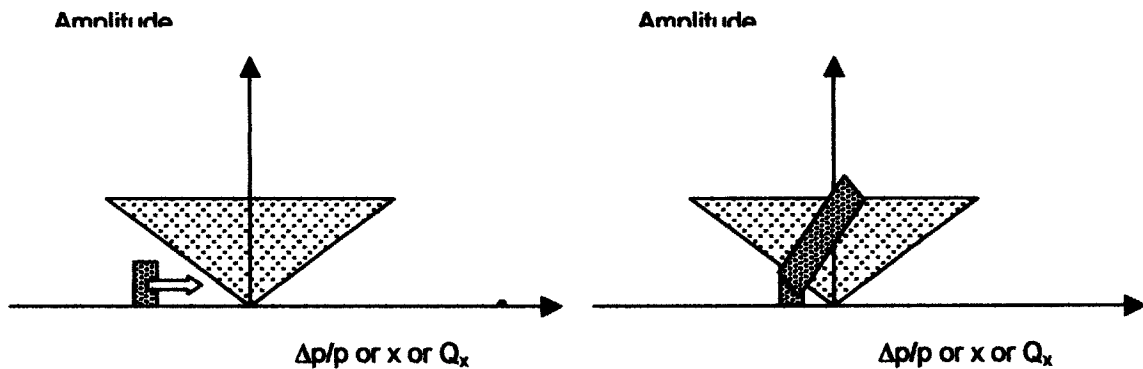


Figure 21 Changing orbit radius

The beam is shown with a narrow energy spread and large betatron amplitude.

The drawback to the previous three selection methods is that the lattice elements are varied during extraction. This may upset the circulating beam and reduce the duration of the spill.

Chapter 5 Slow Extraction Method

We use the rf quadrupole driven at two times the betatron frequency to increase the betatron amplitude. Increasing betatron amplitude will cause the particles to encounter the resonance while maintaining a narrow tune spread. This requires a chromaticity that approaches zero.

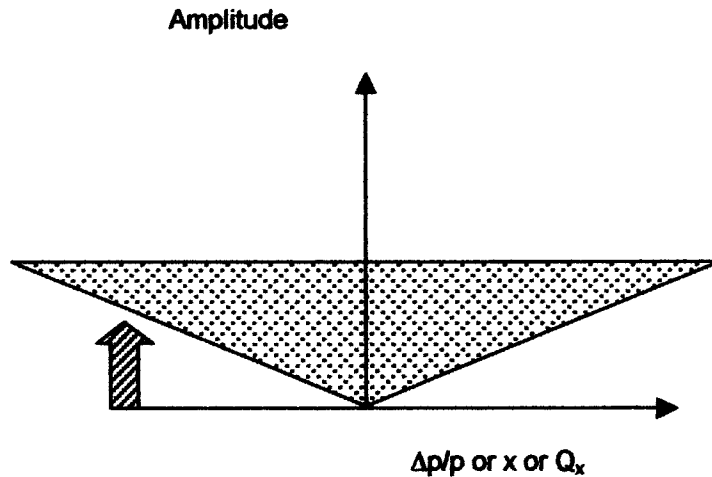


Figure 22 Enlarging beam emittance

Beam is shown with narrow energy spread and variable betatron amplitude. An air core quadrupole driven at a frequency of $2\nu_x$ will be used to excite the betatron motion to larger amplitudes. This will force particles into the separatrix where they are extracted. The RF quadrupole is located in the short straight section with the RF cavity.

Chapter 5 Slow Extraction Method

This stochastic method has the advantage that it does not change the lattice elements. The amplitude of the RF drive will control the spill rate. By increasing the amplitude of the betatron motion with an RF quadrupole, all of the particles in the bunch can be made to encounter the resonance, even particles with very small displacement from the reference orbit.

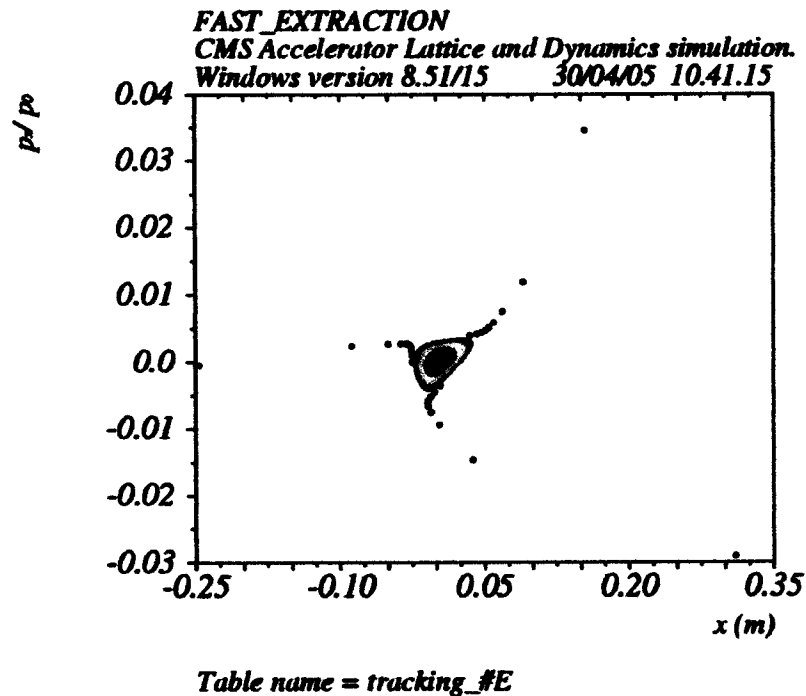


Figure 23 Sextupole and RF Quadrupole activated

Figure shows the horizontal tune set to 1.675 and the sextupole and RF quadrupole activated, the particles with larger amplitudes encounter the separatrix and start to step further away from the stable ellipse.

5.4 Horizontal Electro-Static Wire Septum

The electrostatic septum defines a field-free area for the proton bunch to circulate and an electric field area for deflecting selected particles. A linear array of fine wires (0.05 mm) creates a ground plane defining the two areas. Particles on the separatrix will step over the wires, where a high-voltage electrode attracts them horizontally onto the extraction trajectory.

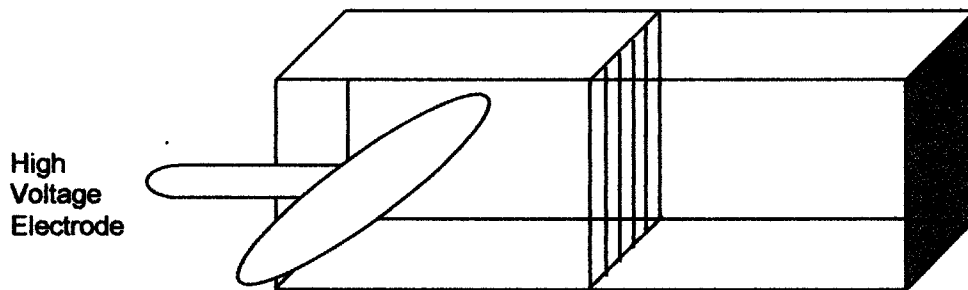


Figure 24 Electro-static septum

Diagram of electro-static septum showing linear array of wires used as ground plane and high voltage electrode.

In contrast with the fast extraction, the fast kicker deflection needed to be large enough to clear the entire bunch width at the magnetic septum. For slow extraction, we only need a deflection large enough for individual protons. The deflection from the electro-static septum is about 12 mm.

Chapter 5 Slow Extraction Method

From table 7 we see that we need a 12 mm displacement at the magnetic septum. The lever arm is 1.9 meters. We use this value to derive the angle as 3.6 mrad.

The electro-static septum parameters are

Electro-static septum		units
length=	1.1	[m]
delta x=	12	[mm]
Lever Arm=	3.9	[mm]
theta=	3.6	[mrad]
Wire diameter	0.05	[mm]
E=	30	[kV]
gap	0.03	[m]

Table 7 Electro-static septum parameters

Extraction efficiency is the ratio of beam radius to the diameter of the septum wires. From Table 3 we have a beam radius of 5.77 mm and wires of 0.05 mm gives 99.2 % extraction efficiency.

6 Conclusions

This thesis presents a detailed description of the extraction system requirements for the Compact Medical Synchrotron (CMS). We describe two distinct methods for extraction of protons from the CMS accelerator, i.e. fast extraction and slow extraction.

In chapter one we described the motivation for this accelerator project. Brief descriptions of the accelerator and extraction concepts are outlined. This accelerator is based upon the successful CIS (Cooler Injector Synchrotron) at IUCF (Indiana University Cyclotron Facility) In chapter two we described the physical characteristics and the operating cycle for the CMS accelerator. In chapter three we examined beam dimensions and machine aperture requirements. The effect of adiabatic damping is considered.

In chapter four we analyzed beam dynamics and described elements needed for the fast extraction process. This method of extraction has applications in scanning radiation treatments. In chapter five we described elements needed for the slow extraction process. This method of slow extraction is particularly well suited to the application of radiation therapy.

Chapter 6 Conclusions

In conclusion, the two extraction methods used for the CMS have many accelerator applications. The primary design application has been radiation therapy treatments. These versatile extraction systems also have possible applications for industry. Due to the strong focusing of a synchrotron lattice, an industrial variant may be an economical alternative to cyclotron based processes e.g. radio-nuclide production.

Bibliography

- [1] S.Y. Lee *Accelerator Physics*, (World Scientific Publishing, Singapore, 1999)
- [2] R. Dilao & R. Alves-Pires *Nonlinear Dynamics in Particle Accelerators* (World Scientific Publishing ISBN 981-02-2517-2)
- [3] Chao & Tigner *Accelerator Physics and Engineering* (World Scientific Publishing, 1999)
- [4] X. Kang, et.al, *Slow Extraction Method for the Cooler Injector Synchrotron*
Indiana University
- [5] X. Kang, et. al., *Beam Extraction System for the Cooler Injector Synchrotron at IUCF* Indiana University
- [6] D.L. Friesel *CIS, A Low Energy Injector for the IUCF* Indiana University
- [7] Nader Al-Harbi, et. al., *Compact Industrial Synchrotron CIS+Indiana University*
- [8] M. (Sanki)Tanaka *MAD Simulation: HEP/SEB Extraction (FY1996)*
AGS/AD/Tech Note No.447
- [9] F. Christoph Iselin *MAD /8.51 (Methodical Accelerator Design)* Geneva,
Switzerland
- [10] S. Humphries, Jr *Charged Particle Acceleration*,(John Wiley and Sons, N.Y. 1986)
- [11] S. Humphries, Jr *Charged Particle Beams* (John Wiley and Sons, N.Y. 1990)
- [12] B.W. Montague *Basic Hamiltonian Mechanics* CERN 77-13, Geneva,
Switzerland

- [13] E.J.N. Wilson *Nonlinear Resonances* CERN 77-13, Geneva, Switzerland
- [14] E. Wilson *Non-Linearities and Resonances* CERN 77-13, Geneva,
Switzerland
- [15] L. Badano, et. al., *Synchrotrons for Hadron Therapy* CERN/PS 99-007
- [16] Lee Teng *Formulas for Resonances of Transverse Oscillations in a Circular
Accelerator* NAL FN-183 2040 March 27, 1969
- [17] S.C. Snowdon *Transformations Useful in Linear Betatron Theory* NAL-185
2040 May 8, 1969
- [18] LOMA LINDA UMC PROTON TREATMENT Loma Linda, CA 92354
- [19] K. Symon *Derivation of Hamiltonians for Accelerators* Argonne National Laboratory
September 1997, ANL/APS/TB-28

Curriculum Vitae

Steven J Daley

Academics

Indiana University/US Particle Accelerator School
Master of Science Beam Physics & Accelerator Technology 2005

Governors State University
Board of Governors Bachelor of Arts 1997

Moraine Valley Community College
Associate of Science Electrical Engineering 1986

Practical Experience

General Electric Healthcare Systems 2001-present
Project Engineer
Maintain and improve RF systems, vacuum, ion source and beamlines for AVF cyclotrons used in radioisotope production

Argonne National Laboratory Physics Division 1992-2002
1996-2002 ATLAS Heavy Ion Linear Accelerator
Maintain & operate ion sources, Tandem Pelletron Vann-de Graff, Superconducting RF Linac. Tune beamline to targets, RF Pulse conditioning, PLC programming Radiation Interlock system manager
1992-1996 Advanced Photon Source 3rd Generation Synchrotron Light Source Operator/Technician commissioned first light

Chicago Tribune Company Freedom Center 1982-1996
Production Support Technician
Facsimile, Telecommunications and Industrial automation support
Laser scanners, microwave & satellite links, PDP-11/VAX, microprocessors

United States Steel Company South Works 1976-1982
Electronics Repairman Apprenticeship/Journeyman